In vitro reconstitution of DNA replication initiated by genetic recombination: a T4 bacteriophage model for a type of DNA synthesis important for all cells

Jack Barry, Mei Lie Wong, and Bruce Alberts*
Department of Biochemistry and Biophysics, University of California, San Francisco, San Francisco, CA 94158-2517

ABSTRACT **Using a mixture of 10 purified DNA replication and DNA recombination proteins encoded by the bacteriophage T4 genome, plus two homologous DNA molecules, we have reconstituted the genetic recombination–initiated pathway that initiates DNA replication forks at late times of T4 bacteriophage infection. Inside the cell, this recombination-dependent replication (RDR) is needed to produce the long concatemeric T4 DNA molecules that serve as substrates for packaging the shorter, genome-sized viral DNA into phage heads. The five T4 proteins that catalyze DNA synthesis on the leading strand, plus the proteins required for lagging-strand DNA synthesis, are essential for the reaction, as are a special mediator protein (gp59) and a Rad51/RecA analogue (the T4 UvsX strand-exchange protein). Related forms of RDR are widespread in living organisms—for example, they play critical roles in the homologous recombination events that can restore broken ends of the DNA double helix, restart broken DNA replication forks, and cross over chromatids during meiosis in eukaryotes. Those processes are considerably more complex, and the results presented here should be informative for dissecting their detailed mechanisms.**

Monitoring Editor
Tom Misteli
National Cancer Institute, NIH

Received: Jun 27, 2018
Revised: Oct 23, 2018
Accepted: Nov 1, 2018

INTRODUCTION

The bacteriophage T4 DNA replication system efficiently replicates this virus's long double-stranded DNA chromosome, and for more than five decades it has served as an effective model for dissecting the detailed mechanisms of DNA replication in all organisms (Liu *et al.*, 1979; Alberts *et al.*, 1983; Mosig, 1983; Nossal and Alberts, 1983; Nossal, 1994; Kreuzer and Brister, 2010; Liu and Morrical, 2010; Benkovic and Spiering, 2017). In the 1980s, an in vitro DNA replication system was developed as an attempt to reconstitute, with purified DNA and proteins, the recombination-dependent form of DNA synthesis that operates during the late stages of T4 bacteriophage infection of *Escherichia coli* cells (denoted as recombination-dependent replication, or RDR). In this system (Formosa and Alberts, 1986), the 3′-OH end of a single-stranded DNA molecule serves as the primer required to start DNA synthesis on a double-stranded DNA template. The reaction requires a double-stranded DNA molecule that has a region complementary to the sequence at the 3′-OH end of the DNA single-strand that primes DNA synthesis, as well as the T4 UvsX strand-exchange protein, a close homologue of the Rad51/RecA proteins (Gajewski *et al.*, 2011). The UvsX protein catalyzes the homologous DNA pairing that forms a displacement loop (D-loop), and it also drives a subsequent ATP hydrolysis–driven directional branch-migration reaction (Yonesaki and Minagawa, 1985; Kodadek and Alberts, 1987; Kodadek *et al.*, 1988; Morrical, 2015). The T4 DNA polymerase holoenzyme is composed of the DNA polymerase (gp43) plus polymerase accessory proteins (the gp45 sliding clamp and the gp44/ gp62 clamp loader; Kelch *et al.*, 2011). This holoenzyme catalyzes DNA synthesis that begins at the 3′-OH end of the DNA primer, in a reaction that requires the T4 single-strand binding protein (gp32, also known as the gene 32-protein; Alberts and Frey, 1970; Kodadek, 1990). This reaction is greatly stimulated by the T4 dda protein, a DNA helicase that binds to a DNA single strand and moves in the 5′ to 3′ direction along it to pry open helical structures (He *et al.*, 2012).

This article was published online ahead of print in MBoC in Press (http://www.molbiolcell.org/cgi/doi/10.1091/mbc.E18-06-0386) on November 7, 2018.

*Address correspondence to: Bruce Alberts (balberts@ucsf.edu).

Abbreviations used: D-loop, displacement-loop; gp41, T4 gene product 41; gp59, T4 gene product 59; gp61, T4 gene product 61; HSA, human serum albumin; RDR, replication-dependent replication.

Because branch migration driven by the UvsX protein can remove the newly synthesized DNA chain from its template behind the polymerase, the above system produces a moving "replication bubble," with a newly made single-stranded DNA molecule being released as the final product. Specific protein–protein interactions are required, inasmuch as the *E. coli* RecA protein is unable to substitute for the UvsX protein in this in vitro reaction, with or without *E. coli* SSB present (Formosa and Alberts, 1986). This form of DNA synthesis is said to be conservative, in contrast to the semiconservative form of DNA synthesis that is catalyzed by a standard replication fork. (As for RNA synthesis, the DNA double helix that serves as the template is left unchanged.)

The T4 gene 41 protein (gp41) is a DNA helicase that interacts with a DNA primase (61 protein, gp61) to form the T4 primosome on the lagging strand of a replication fork (Cha and Alberts, 1986; Hinton and Nossal, 1987; Jing *et al.*, 1999; Zhang *et al.*, 2005: Lee *et al.*, 2013). The addition of these two proteins had no effect on the recombination-dependent DNA synthesis reactions previously reported (Formosa and Alberts, 1986). Subsequently, the T4 gene 59 mediator protein (gp59) was discovered and characterized (Yonesaki, 1984; Barry and Alberts, 1994; Morrical *et al.*, 1994, 1996); gp59 binds to both gp41 and gp32, and it thereby promotes the assembly of the T4 primosome on DNA (Jones *et al.*, 2001; Ma *et al.*, 2004; Delagoutte and von Hippel, 2005; Branagan *et al.* 2014; Benkovic and Spiering, 2017). The gp59 mediator (also termed a helicase-assembly protein) is required for efficient recombination-dependent DNA replication inside a T4 bacteriophage-infected cell (Shah, 1976), and in this report we reexamine the properties of the above in vitro DNA replication system with this protein present.

T4 bacteriophage, which was selected by Max Delbrück and the phage group to initiate the new field of molecular biology in the early 1940s (Strauss, 2017), is now known to have many relatives in the ocean that infect the enormously abundant marine cyanobacteria of the genera *Synechococcus* and *Prochlorococcus* (Filée *et al.*, 2005). As a major component of the many different viruses that, in total, are estimated to kill ~20% of the total ocean biomass per day, these cyanophages play a large role in nutrient recycling (Suttle, 2007). Thus, quite unexpectedly, the proteins studied here—which are conserved in these T4 relatives (Clokie *et al.*, 2010)—intimately affect the Earth's ecology.

RESULTS

The gp59 mediator promotes T4 primosome assembly on single-stranded DNA covered with the gp32 and UvsX proteins

At late times of infection of an *E. coli* bacterium by T4 bacteriophage, the replication of the viral DNA is initiated by a process that requires genetic recombination (Luder and Mosig, 1982; Mosig, 1983). The T4 strand-exchange protein, UvsX, is essential for this synthesis, and abundant amounts of this protein are produced (Yonesaki and Minagawa, 1985). This DNA-dependent ATPase, a Rad51/RecA analogue, binds tightly and cooperatively to a DNA single strand in the presence of ATP. It thus forms long clusters that hold DNA in a special elongated conformation that can extend for thousands of DNA nucleotides (Harris and Griffith, 1987; Ando and Morrical, 1998; Gajewski *et al.*, 2011).

A moving DNA replication fork requires a DNA helicase enzyme that uses the energy of nucleoside triphosphate hydrolysis to pry open the DNA double helix ahead of the leading-strand DNA polymerase. For T4 bacteriophage, this helicase is gp41, which forms the T4 primosome along with a partner DNA primase (gp61). The loading of this helicase—and thus the primosome—onto DNA is an important step in forming a replication fork. Rates of gp41 loading can be readily measured in vitro by assaying for the primosome-dependent initiation of RNA-primed DNA synthesis on a single-stranded circular DNA template, as schematically illustrated in Figure 1D (Cha and Alberts, 1986; Hinton and Nossal, 1987). Under conditions resembling those inside a cell, where an excess amount of gp32 is present to coat DNA single strands, gp41 loading is greatly accelerated by the addition of the gp59 mediator (Jones *et al.*, 2001; Ma *et al.*, 2004; see also Figure 1A). However, as shown in Figure 1B, there is no detectible loading of gp41 onto DNA when the UvsX protein alone coats single-stranded DNA, either with or without gp59 present.

What happens to helicase loading when both gp32 and UvsX protein are present in a roughly 1:1 mixture, and in excess over the available single-stranded DNA—the situation that exists within a T4-infected cell? As shown in Figure 1C, without the gp59 mediator present, gp41 loading is nearly completely blocked; but when gp59 is added, gp41 loading is restored to nearly the rate observed without UvsX protein present (a 23-fold increase in rate; compare Figure 1A with Figure 1C). To interpret this result, we note that, when both UvsX and gp32 are present in excess, the two compete for binding to a DNA single strand. Because each protein binds cooperatively to DNA, with a gp32 monomer preferring to bind next to a previously bound gp32 molecule and a UvsX monomer preferring to bind next to a bound UvsX molecule, long alternating clusters of each type of protein are observed on a single–stranded DNA molecule (Griffith and Formosa, 1985). As others have studied in detail (Jones *et al.*, 2001; Branagan *et al.*, 2012, 2014), gp59 binds both to gp32 and to gp41, and it can act as a mediator to load gp41 onto patches of DNA covered with gp32. The results in Figure 1C demonstrate that this loading also occurs efficiently in the presence of excess UvsX protein. But from the Figure 1 results, we conclude that gp41 loading can only occur on those regions of single-stranded DNA that have gp32 bound, and that any regions covered with UvsX protein are not accessible targets in our system (note that the T4 UvsY protein was not present in these experiments; for a more complete analysis with similar conclusions, see Bleuit *et al.*, 2001).

Once begun, the DNA synthesis catalyzed by the T4 DNA polymerase holoenzyme appears to have little or no problem using a UvsX-coated single strand of DNA as its template. If there were such a problem, the rate of DNA synthesis with 59 protein present in Figure 1C should be much less than is observed.

The addition of the gp59 mediator strongly stimulates recombination-dependent DNA synthesis in an in vitro assay

The above results encouraged us to add 59 protein to the in vitro assay system that had been explored in detail earlier. In our version of the assay, a unique single-stranded DNA fragment of 1623 nucleotides is provided to prime DNA synthesis on a 7.25-kb linear double-stranded DNA molecule that contains a complementary sequence. Aided by a small amount of the T4 mediator protein UvsY (also termed a recombination-mediator protein), the T4 UvsX strand-exchange protein coats this single strand and catalyzes a DNA pairing reaction that inserts the 3′-OH end of this "primer" into a homologous region of the double-stranded DNA, forming a D-loop. The inserted 3′-OH end then primes DNA synthesis by the T4 DNA polymerase holoenzyme, which uses the double-stranded DNA as a template.

What DNA products might be expected to form in our in vitro reactions? In the absence of a complete T4 primosome (that is, when either gp61 or gp41 protein is missing), our earlier results indicate that a DNA single strand should be produced through a

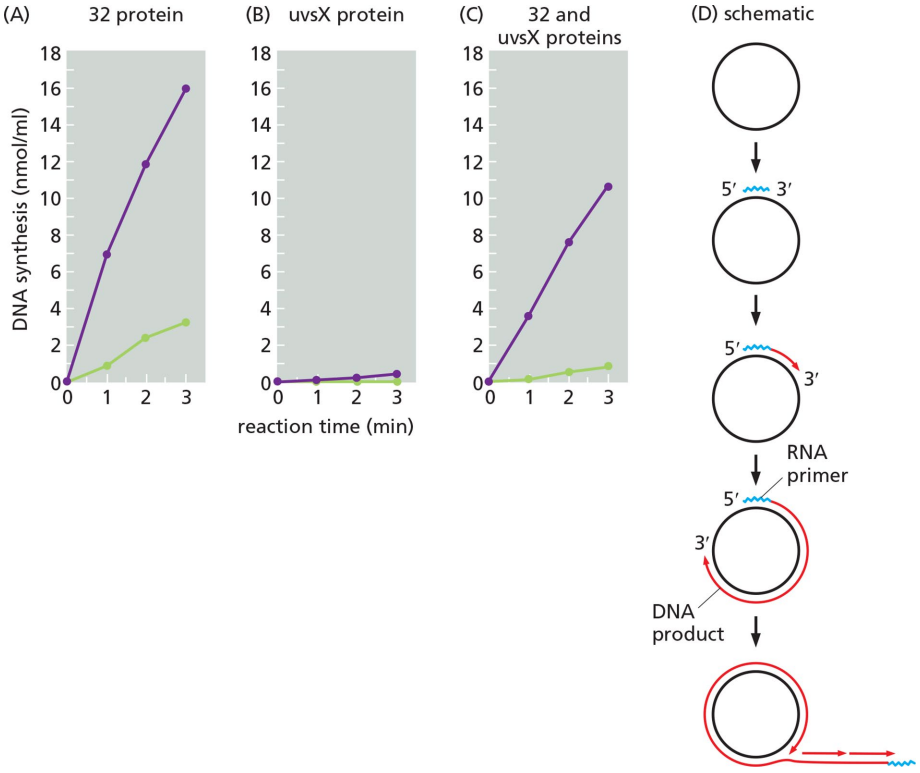

FIGURE 1: In the presence of UvsX protein, both gp59 and gp32 (32 protein) are needed to assemble a primosome on single-stranded DNA. RNA-primed DNA synthesis was carried out as described in *Materials and Methods*, either with (purple) or without (green) the addition of gp59. The single-stranded, circular M13 DNA template was incubated for 1 min at 37°C with the following DNA binding proteins: (A) gp32 (32 protein), (B) UvsX protein, and (C) both gp32 and UvsX proteins. DNA synthesis was then initiated by the addition of the T4 DNA polymerase holoenzyme and the T4 primosome (the DNA primase, gp61, plus the DNA helicase, gp41). When present, gp32 was present at 1.2 times the amount needed to cover all the single-stranded DNA (62 μg/ml), based on a binding site of 7 nucleotides per gp32 molecule (Jensen *et al.*, 1976). The UvsX protein was present at 1.3 times the amount needed to cover all the single-stranded DNA (100 μg/ml), based on a binding site of five nucleotides per UvsX protein molecule. In (C) many DNA circles are covered by alternating patches of UvsX and gp32, each in a linear array that reflects each protein's cooperative DNA binding (Griffith and Formosa, 1985). In (D), we diagram the sequence of polynucleotide syntheses in these reactions—the primosome-catalyzed synthesis of a pentaribonucleotide (RNA primer) that then primes DNA synthesis by T4 DNA polymerase and its accessory proteins.

mechanism that involves a moving replication bubble (Formosa and Alberts, 1986). This conservative form of DNA synthesis is diagrammed on the left side of Figure 2, and it should proceed whether or not gp59 is added.

With both primosome and gp59 mediator present, DNA should still be synthesized continuously on one template strand, resembling the DNA made on the leading strand of a fork. But short DNA fragments should now be made on the other template strand, reflecting a repeated production of short RNA primers that repeatedly initiate DNA synthesis (just as for the "Okazaki fragments" synthesized on the lagging side of a normal replication fork). Very importantly, as illustrated on the right side of Figure 2, there are two very different pathways for such synthesis. If the primosome loads onto the long, emerging single-stranded DNA tail, a conservative form of double-stranded DNA synthesis results; in contrast, if the primosome loads onto the single-stranded DNA *inside* of the D-loop bubble, double-stranded DNA is synthesized semiconservatively.

Figure 3 provides an analysis of the DNA produced in our new in vitro reactions. Because agarose gel electrophoresis in 30 mM NaOH has been used to separate the two strands of all DNA double helices present, a gel autoradiograph reveals the size of the newly synthesized DNA strands (radioactively labeled due to the [α-^{32}P]dTTP precursor). In most reactions, the predominant product is a DNA strand of ~7162 nucleotides, as expected from full elongation of the primer strand (the 7250-nucleotide template length minus 88 nucleotides). Short Okazaki fragments are produced only when both of the proteins that form the T4 primosome are present (gp41 and gp61), along with gp59 (reaction 6 in Figure 3). (Note that, because the enzymes that remove RNA primers inside the cell are absent in our reactions, each Okazaki fragment remains disconnected from its neighbors.) As extensively studied elsewhere, these fragments are greatly reduced if rUTP and rCTP are omitted from such in vitro reactions, inasmuch as these precursors are required to synthesize most T4 pentaribonucleotide primers (Liu and Alberts, 1980, 1981).

The addition of the gp61 DNA primase alone is without effect on the products obtained, with or without gp59 present. But in a reaction requiring gp59, the addition of the gp41 DNA helicase alone stimulates DNA synthesis—significantly increasing the amount of radioactive label in the largest (slowest-migrating) DNA strands (compare reaction 4 to reaction 2 in Figure 3).

We next repeated critical parts of the experiment using a 5′ ^{32}P end-labeled, 1623-nucleotide DNA single strand to prime DNA synthesis, leaving all of the deoxyribonucleoside triphosphate precursors unlabeled. In this case, an exclusive labeling of the DNA made on the leading strand is expected from either of the alternative models on the right side of Figure 2. The results are shown in Supplemental Figure S1. As expected, the quantity of short radioactive DNA strands is greatly reduced compared with that in Figure 3 (and is here attributed to incompletely lengthened 1623 nucleotide primers). Moreover, the addition of gp61 to gp41 (to complete the primosome) now has little effect on the pattern of radioactivity observed by gel electrophoresis, inasmuch as the Okazaki fragments being produced are not radioactive.

Supplemental Table S1 describes how the rate and products of the complete reaction in Figure 3 (reaction 6) change when other specific DNA and protein components are omitted. The table reveals that the dda DNA helicase, which is present in nearly all of the experiments that we report here, has no effect on the pattern of DNA products produced. This helicase was strongly required for recombination-induced DNA synthesis in earlier studies (Formosa and Alberts, 1986); but with the gp41 helicase now engaged, the dda helicase stimulates synthesis only ~1.5-fold.

When the primosome is active, the longest DNA products in Figure 3 and in Supplemental Figure S1 have a length of ~7 kb, as expected from the reactions diagrammed in Figure 2. However,

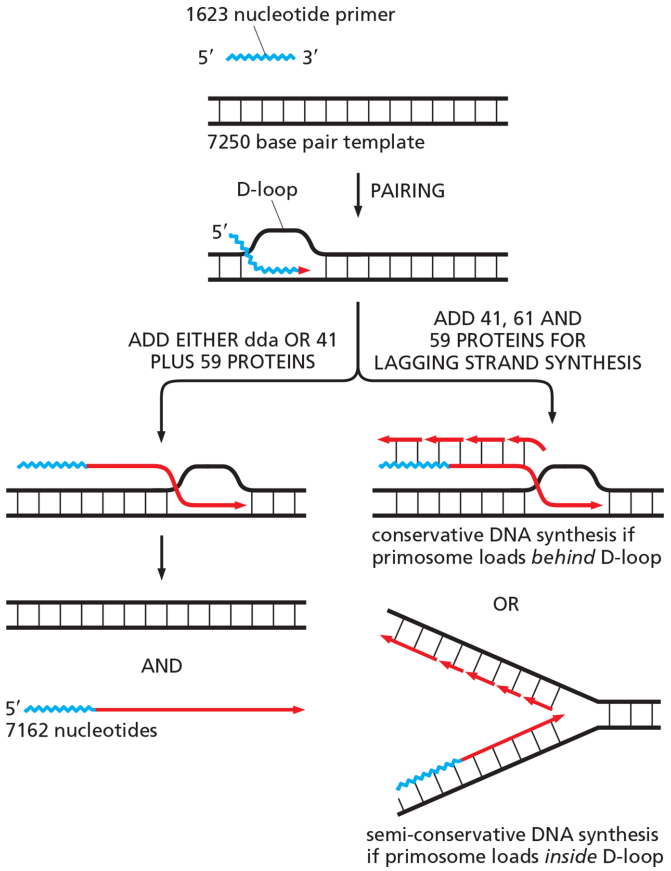

FIGURE 2: Schematic illustration of three possible types of recombination-dependent DNA synthesis. (Left) Conservative DNA synthesis of the type reported by Formosa and Alberts (1986), in which only a DNA single strand is produced. The dda protein was the T4 DNA helicase used in that earlier work; here we show that we can replace it with a mixture of gp41 DNA helicase and gp59 to drive the reaction shown on the left. (Right) Top, What happens when gp61 is added to form a complete primosome? If the T4 primosome (gp41 plus gp61) is loaded onto the displaced single-stranded tail, conservative DNA synthesis will produce a new DNA double helix in which both of the DNA strands in the new duplex are newly made. Bottom, If the T4 primosome is instead loaded inside the D-loop, DNA synthesis will occur semiconservatively. In that case, as at the standard replication fork, both of the two daughter DNA helices produced contain one old and one new strand.

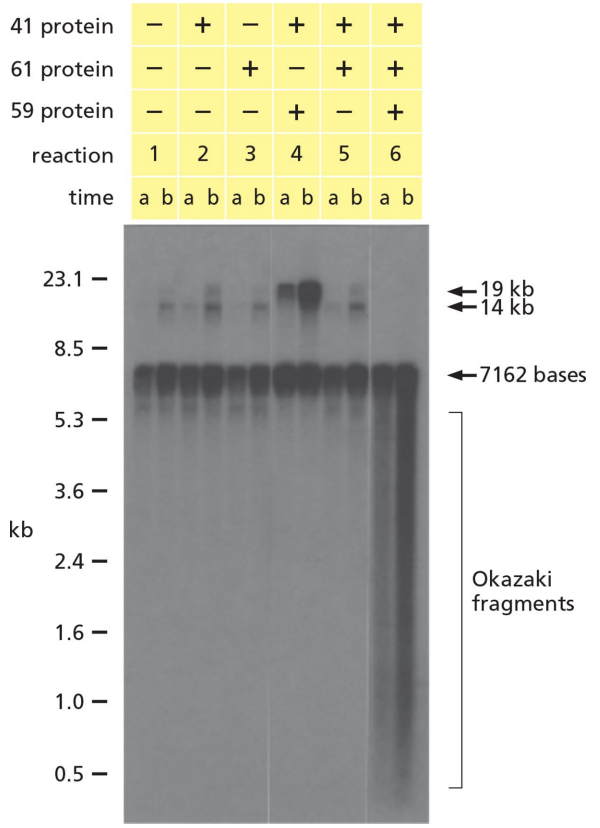

FIGURE 3: Okazaki fragments are produced during recombination-dependent DNA synthesis only when both gp59 and the primosome are present. As diagrammed in Figure 2, the 1623-nucleotide-long single strand that primes recombination-dependent DNA synthesis is homologous to a region that begins 88 nucleotides from one end of a *Bgl*II linearized DNA template (which contains 7250 nucleotide pairs). DNA synthesis that is primed by the 3′OH end of the single strand can therefore extend this strand by 5539 nucleotides to the end of the double-stranded template, producing a 7162-nucleotide-long DNA single strand as product (7250 minus 88 nucleotides). In reactions 1 through 5 there is no functional primosome, and "snap-back" DNA synthesis (Goulian *et al.*, 1968; Englund, 1971) on the 7-kb single-stranded DNA product is seen to produce small amounts of a hairpin helix formed from a DNA strand elongated to 14 kb (see Supplemental Figure S5A and Morrical *et al.*, 1991). The addition of the 41 protein (gp41), a DNA helicase that moves in the 5′ to 3′ direction along a DNA single strand, stimulates snap-back synthesis; but it also produces a small amount of more slowly migrating DNA strands (henceforth designated as "19 kb"). The latter reaction, which is greatly increased by addition of gp59, is eliminated when the primosome is activated to produce Okazaki fragments on the single-stranded DNA (reaction 6). Standard reactions for recombination-dependent DNA synthesis were prepared as described in *Materials and Methods*. Linearized M13MP19 double-stranded DNA (prepared by *Bgl*II digestion) was preincubated with the DNA polymerase holoenzyme, gp32, the dda DNA helicase, and the recombination proteins UvsX and UvsY. The 61 protein (gp61 DNA primase), 41 protein (gp41, DNA helicase), and 59 protein (gp59) were present where indicated. After a brief equilibration at 37°C, recombination-dependent DNA synthesis was started by the addition of a linear single-stranded DNA molecule and the nucleotide substrates (see *Materials and Methods*). After different times at 37°C, the mixture was subjected to strong denaturing conditions and the radioactivity in the individual DNA strands produced, labeled by incorporation of [α-^{32}P]dTTP at 830 Ci/mol, was analyzed by electrophoresis through a 0.8% agarose alkaline gel. An autoradiograph of the gel is shown at the (a) 10-min and (b) 20-min time periods.

when primosome assembly is blocked, some single-stranded DNA products are synthesized that appear to be much longer than the linear double-stranded DNA template. More specifically, in reaction 2 of Figure 3, a small amount of labeled DNA is seen to be produced with an apparent size of 14 kb, twice the 7-kb length. There is nothing surprising here: a product of this length is readily generated if the 3′OH end of a released 7-kb single strand folds back on itself to form a short hairpin helix—thereby allowing its 3′OH to prime "snap-back" DNA synthesis on that same strand. The expected product is a 7-kb double-stranded DNA molecule with its two strands covalently linked at one end, which migrates as a 14-kb single strand during alkaline agarose gel electrophoresis (see Supplemental Figure S5A). However, DNA strands are also detected that migrate more slowly, and more heterogeneously, at approximately 19 kb. This product becomes quite significant only when both gp41 and gp59 are present (see reaction 4 of Figure 3). As is true for the 14-kb band, the "19-kb" species is eliminated when

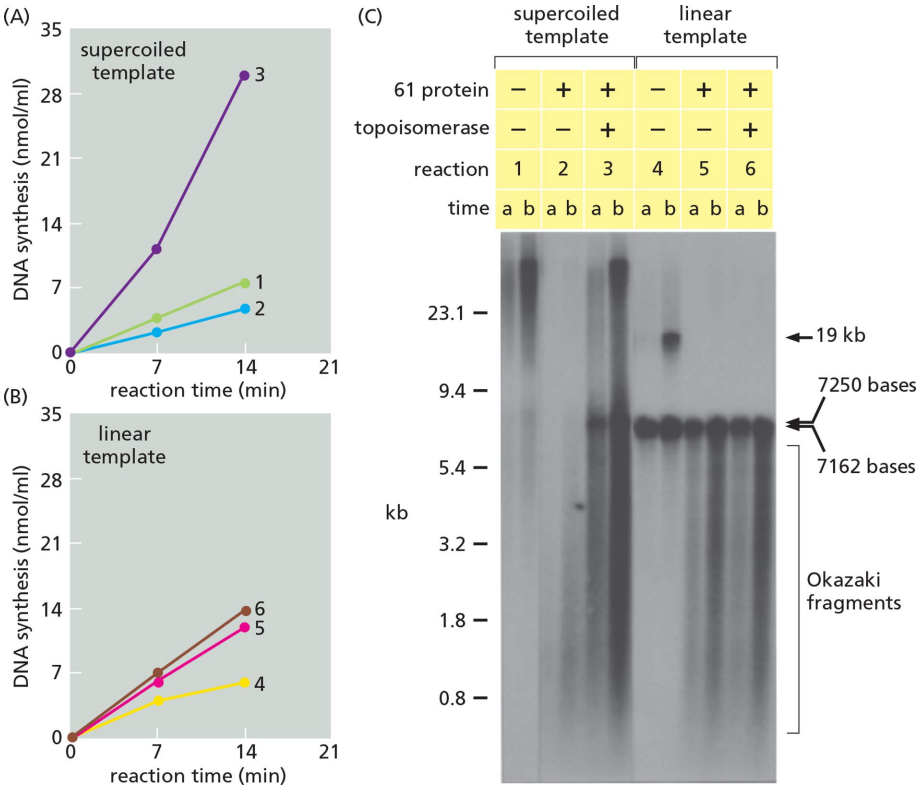

FIGURE 4: Lagging-strand DNA synthesis creates a DNA topoisomerase requirement for recombination-dependent DNA synthesis on supercoiled, but not on linear DNA templates. (A) Amount of DNA synthesized when the double-stranded DNA template is supercoiled. (B) Amount of DNA synthesized under exactly the same conditions when the double-stranded DNA template is linear. (C) Alkaline agarose gel electrophoresis of the radioactive products from the reactions in A and B. Note that DNA products much longer than the supercoiled template molecule are formed in the absence of gp61 and topoisomerase (reaction 1), due to rolling-circle DNA synthesis from a small moving bubble (Formosa and Alberts, 1986). But when gp61 is added to complete the primosome, lagging-strand synthesis occurs on the supercoiled template. Now all of the products are short without topoisomerase present (reaction 2). When topoisomerase is added, long DNA products are synthesized on the supercoiled template like those in reaction 1, along with products resembling Okazaki fragments and a conspicuous band at 7.25 kb (reaction 3). In contrast, there is no effect of topoisomerase on the products made on the linear template in the presence of 61 protein (compare reactions 5 and 6). See Figure 5 for diagrams that illustrate these results. As described in *Materials and Methods*, M13MP19 double-stranded DNA, either supercoiled (form I) or *Bgl*II-linearized (form III), was preincubated with the DNA polymerase holoenzyme, gp32, gp41, gp59, UvsX, UvsY, and the dda DNA helicase. The gp61 DNA primase (61 protein) and the T4 DNA topoisomerase were also present where indicated. After temperature equilibration at 37°C, recombination-dependent DNA synthesis was started by the addition of the homologous 1623 nucleotide single-stranded DNA primer and the nucleotide substrates. After 7 and 14 min of DNA synthesis, the amount of product was determined from the incorporation of radioactively labeled [α-^{32}P]dTTP precursor (panels A and B), and aliquots were analyzed by alkaline gel electrophoresis through 0.6% agarose followed by autoradiography (panel C).

Okazaki fragments are synthesized (compare reactions 4 and 6 in Figure 3, or reactions 1 and 2 in Supplemental Figure S1). For a discussion and diagram that illustrate how this unexpected product can arise, see the Supplemental Text and Supplemental Figure S5.

The T4 primosome rapidly loads inside a D-loop bubble, producing semiconservative DNA replication

The results presented thus far are consistent with either of the two modes of recombination-dependent DNA synthesis that were illustrated on the right side of Figure 2—that is, with either the conservative or the semiconservative synthesis of a new DNA double helix. To distinguish between these two very different reactions, we replaced the linear DNA double helix that serves as the template in Figure 3 with a closed circular supercoiled DNA molecule. Recombination-dependent DNA synthesis by the conservative mechanism should be unaffected by this change. But if the semiconservative mechanism of synthesis occurs instead, DNA synthesis should be blocked soon after it starts by a rapid increase of superhelical tension ahead of the new replication fork that forms. Moreover, because the addition of a DNA topoisomerase enzyme can release all such tension, topoisomerase addition would be expected to stimulate DNA synthesis only for the semiconservative mechanism.

We compare the amount of recombination-dependent in vitro DNA synthesis observed on a linear versus a circular, supercoiled DNA template molecule in Figure 4, A and B. On a linear DNA template, twice as much DNA is synthesized when gp61 (61 protein) is added to complete the primosome (compare reaction 5 with reaction 4 in Figure 4B), as expected for the induction of DNA synthesis on the lagging strand. But when the same DNA template is present in a closed circular form, completing the primosome inhibits DNA synthesis (compare reaction 2 with reaction 1 in Figure 4A). Most strikingly, the addition of T4 DNA topoisomerase (a complex of T4 gp39/gp52/gp60) converts this inhibition into a dramatic stimulation of DNA synthesis by gp61 addition (compare reaction 3 with reaction 2 in Figure 4A). These findings support the *semiconservative* mechanism of DNA synthesis that was illustrated in Figure 2.

A comparison of the size of the DNA product strands, analyzed by agarose gel electrophoresis under DNA-denaturing conditions, supports this conclusion. As shown in Figure 4C, a very long leading-strand product is seen to be produced by "rolling circle" DNA synthesis on the circular, supercoiled DNA template in the absence of the primosome (reaction 1). The synthesis of this product is completely blocked when gp61 is added to complete the primosome (reaction 2). But with topoisomerase present, this block is converted to strong gp61 stimulation, accompanied by abundant Okazaki fragment synthesis (reaction 3).

Our interpretation of the reactions observed on a circular, supercoiled DNA template molecule is diagrammed in Figure 5. As it does on a linear double-stranded template, the reaction starts with the UvsX protein-catalyzed insertion of the 3'OH end of the 1623-nucleotide primer into the region of DNA double helix of complementary sequence, forming a "D-loop bubble." Inside this bubble, a section of the double-stranded template molecule is exposed as a single strand, having been displaced by the invading

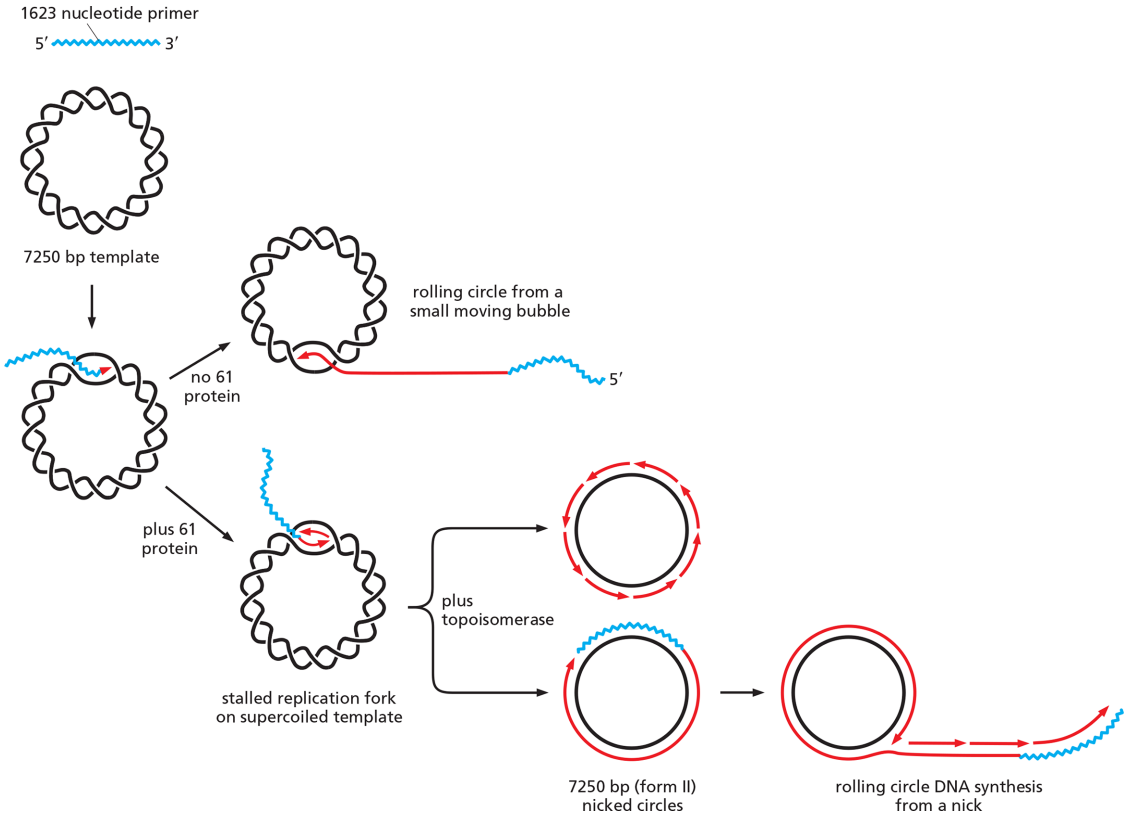

FIGURE 5: Depiction of the products of recombination-dependent DNA synthesis on a supercoiled template. The products of reactions 1–3 in Figure 4 can be accounted for by the molecules shown here. For simplicity, supertwisted molecules are depicted in the covalently closed relaxed state. Because lagging-strand synthesis is semiconservative, the replication fork stalls when topoisomerase is not present to remove DNA winding strain ahead of the fork. The replication fork in the plus-topoisomerase reaction is depicted as unidirectional. Consequently, one of the form II circular products of this reaction contains a newly synthesized leading strand that is 7250 nucleotides long.

DNA primer. The unfavorable free energy of positive supercoiling is expected to limit the length of this single strand to only a few hundred nucleotides (Wang, 1969). To explain the semiconservative DNA synthesis observed in the complete reaction, the primosome must be rapidly and preferentially loaded onto this small region of single-stranded DNA. Once so positioned, the primosome produces a 5-nucleotide-long RNA primer that initiates Okazaki fragment production inside the bubble (Liu and Alberts, 1980; Cha and Alberts, 1986; Hinton and Nossal, 1987).

On a circular, superhelical DNA template, the leading-strand DNA polymerase is quickly forced to stop due to the superhelical tension that builds up as it moves, requiring a topoisomerase to relieve the tension. In contrast, without the complete primosome (that is, without gp61 added in our experiments), no Okazaki fragments are synthesized. Now the superhelical tension that DNA synthesis creates is removed by strand displacement at the back of the D-loop, aided by UvsX protein (Yonesaki and Minagawa, 1985; Kodadek and Alberts, 1987; Kodadek *et al.*, 1988; Morrical, 2015). This allows a long DNA single strand to be synthesized by a conservative mechanism (rolling circle replication from a small moving bubble), even with no topoisomerase present (see Formosa and Alberts, 1986).

In the presence of a DNA topoisomerase, the scheme diagrammed in Figure 5 predicts a nicked double-stranded DNA circle as a major product of the recombination-dependent DNA synthesis that occurs on a circular double-stranded DNA template. To test this prediction, we analyzed the products of the reaction by electrophoresis through an agarose gel at neutral pH, a condition that leaves the DNA double helix intact. The results demonstrate the formation of the expected 7.25-kb M13MP9 form II nicked circle, in a reaction that requires both a DNA topoisomerase and the complete T4 primosome (Figure 6).

The Supplemental Material presents further information on the properties of this reaction. As expected, the topoisomerase-dependent DNA synthesis observed on a supercoiled circular template requires both a single-stranded DNA primer and the UvsX protein (Supplemental Figure S2). Replacing the radioactive deoxyribonucleoside triphosphate with a radioactively labeled primer strand as the only labeled precursor reveals that the reaction starts asynchronously, requiring 16 min for the majority of primer strands to be used to start DNA synthesis (Supplemental Figure S3). (Note that the number of template molecules exceeds the number of primer molecules in our reactions; see *Materials and Methods*.)

Electron microscopy of the DNA products produced on a circular, supercoiled template

We have used electron microscopy to analyze the DNA products present after 7 min of synthesis in the two reactions in Figure 6 that contain a functioning primosome (reaction 2, without topoisomerase, and reaction 3, with topoisomerase). The DNA spreading techniques used allow single- and double-stranded regions of DNA to be readily distinguished in individual DNA molecules (see *Materials and Methods*), and by randomly selecting fields containing hundreds of molecules, we could estimate the relative abundance of

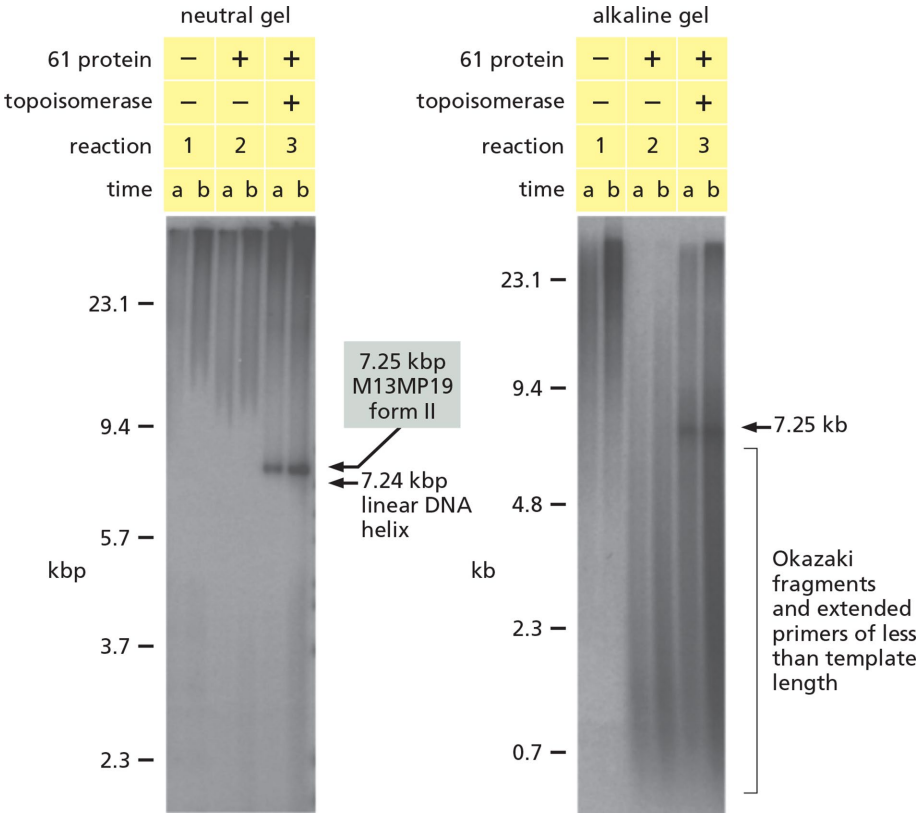

FIGURE 6: A major product of topoisomerase-dependent recombination-dependent DNA synthesis on the supercoiled M13MP19 (form I) template is a discrete band identified by electrophoresis on neutral gels as nicked M13MP19 (form II) double-stranded circles. Only those reactions with gp61 (61 protein) contain an active primosome. DNA synthesis on a supercoiled DNA template was carried out exactly as described for reactions 1–3 in Figure 4. Reactions were stopped with cold EDTA as described in *Materials and Methods.* Aliquots were then split and processed either for electron microscopy (see Figure 7) or gel electrophoresis. Shown here are autoradiographic analyses of the radioactive DNA products after electrophoresis on an alkaline 0.6% agarose gel (right) and a 0.8% agarose gel at neutral pH (left), following (a) 7 min and (b) 14 min of reaction. As seen previously, DNA synthesis in reaction 2 (no topoisomerase) is remarkably limited in comparison with the synthesis observed in the presence of topoisomerase (reaction 3). Most of the products of these DNA synthesis reactions move slowly in their native state on the neutral gel and are indistinguishable from one another. The exception is the prominent band in reaction 3, identified as the M13MP19 (form II) nicked circle by direct comparison with a randomly nicked M13MP19 DNA standard. Form II of M13MP19 is a predicted product of topoisomerase-dependent, semiconservative DNA synthesis (see Figure 5). The slowly moving products on the neutral gel include the DNA networks ("aggregates") that form when UvsX, double-stranded DNA, and homologous single-stranded DNA react (see Formosa and Alberts, 1986). Also running slowly on the neutral gel are "rolling circle" molecules (molecules undergoing either strand displacement synthesis initiated from a nick or DNA synthesis from a small moving bubble), as well as positively supertwisted circles with a stalled replication bubble, whose unique structure apparently causes them to move slowly. (In contrast, simple circular molecules that are negatively or positively supertwisted run faster than nicked circles on the neutral gel.) Minor products detected in the neutral gel of size 1–5 kbp (reaction 3b) are thought to be single-stranded Okazaki fragments, displaced from their lagging strand template by "onion skin" DNA synthesis. The products made in reactions 2 and 3 are analyzed by electron microscopy in Figure 7.

products with different DNA structures. Figure 7 presents the data for each class of molecule that constituted more than 10% of the product from at least one of the two reactions. Micrographs that illustrate these six major classes are shown in Figure 7, A–F, accompanied by the percentages observed for each class in the plus-topo and minus-topo reactions, which are also plotted in Figure 7G.

In the presence of topoisomerase, the major product observed is the open form II circle (Figure 7D), in agreement with Figures 5 and 6. The rolling circle product that is also predicted in Figure 5 ("rolling circle DNA synthesis from a nick") is four- to five-fold less abundant in terms of molecule numbers (12% vs. 55%t of molecules; Figure 7E). Replication forks that create such rolling circles can be generated by our T4 DNA replication system once a nicked circular DNA template (e.g., the form II circle) is present (Morris *et al.*, 1975; Nossal and Peterlin, 1979; Sinha *et al.*, 1980).

As we would expect, the products of recombination-dependent DNA synthesis are quite different in the absence of DNA topoisomerase. About 15% of the molecules visualized were in the form of highly twisted DNA circles (Figure 7C), as predicted from the stalled replication bubble drawn in Figure 5. Only 8% of the molecules in the sample were the open form II circles that constitute 55% of the molecules in the plus-topo reaction, an amount that could have been generated by a simple nicking of the supercoiled template (Figure 7D).

A surprise is the molecules that could be generated by conservative synthesis of a DNA double helix: that is, circular template molecules with a D-loop from which a double-stranded tail emanates (Figure 7B). These molecules are only 2% of the total in the plus-topo reaction, but constitute 25% in the minus-topo reaction. How might we explain this finding? A clue comes from the observation that the double-stranded tails were short, over 90% being shorter than the template length after 7 min of reaction, with a majority less than one-fourth template length (that is, less than 1.8 kb). For a reaction in which a long rolling-circle tail produced by bubble migration is simply filled in with Okazaki fragments under conditions of primosome activation (the conservative DNA synthesis model in Figure 2), DNA tails more than 25 kb in length would be expected (e.g., see reaction 1 in Figure 4C). Both our electron microscope results and the agarose gel electrophoresis data show that something very different is involved, inasmuch as there is only a tiny amount of leading-strand synthesis when the primosome is active without topoisomerase present. (Reaction 2 in Supplemental Figure S3 reveals leading strand lengths of 2 to 3 kb at 8 min, with a small minority of strands creeping up to 5–7 kb by 16 min.)

Our explanation for the DNA product observed in Figure 7B is that diagrammed in Figure 8. After the leading-strand DNA polymerase stops moving due to the superhelical tension that builds up on a closed circular DNA template, a branch migration process *behind* the site of polymerase action can slowly remove this tension.

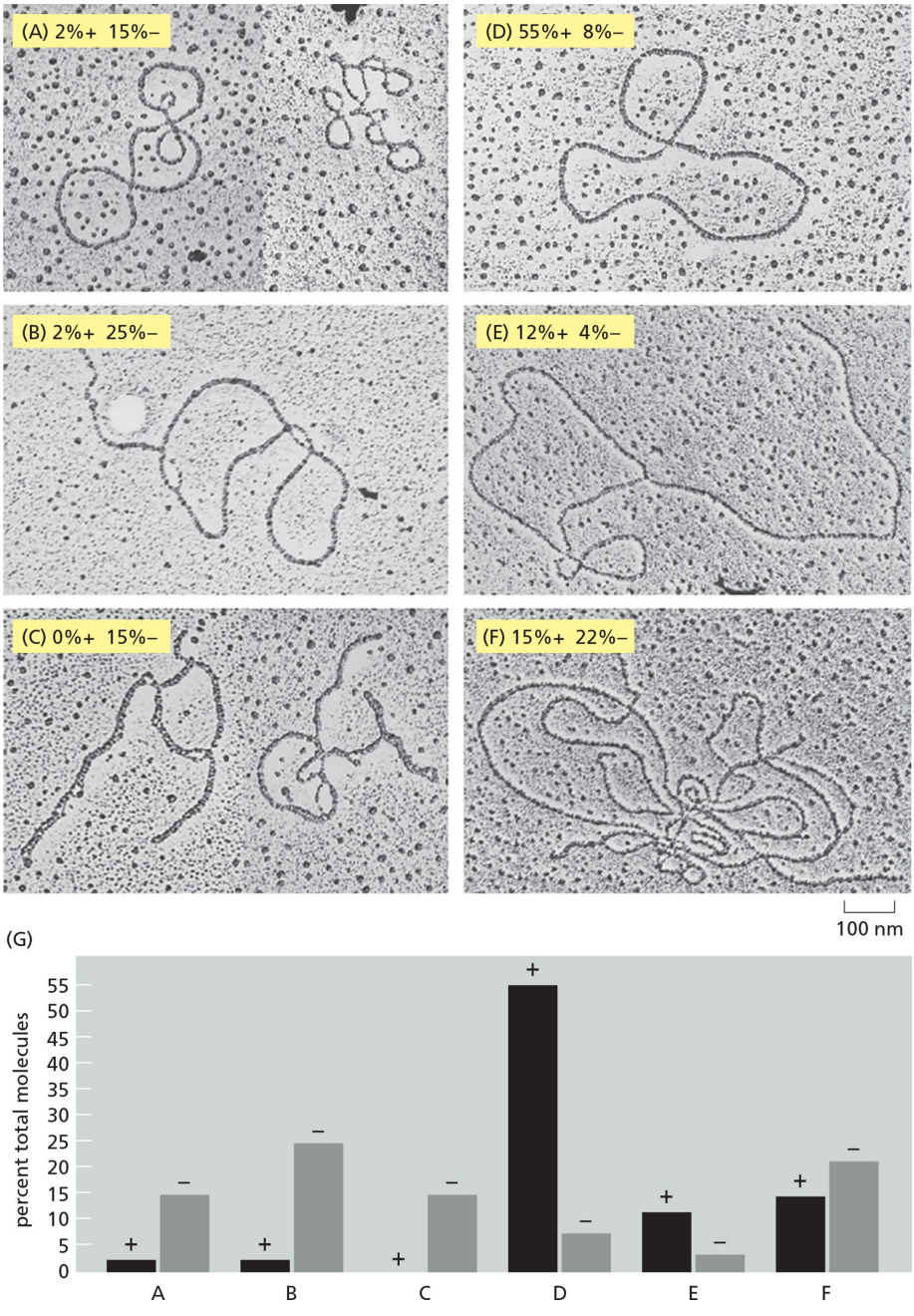

FIGURE 7: Electron microscopy confirms and extends the conclusions derived from biochemical analyses. The DNA products present after 7 min of synthesis in the two reactions in Figure 6 containing gp61 and thus a complete primosome (reaction 2 without topoisomerase and reaction 3 with topoisomerase) were examined by electron microscopy. Aliquots from each reaction were spread on electron microscope grids (see *Materials and Methods*), and all visible molecules of each type were scored by sampling areas of equivalent size on each of six grids. In total, 362 molecules from reaction 2 (minus topoisomerase) and 619 molecules from reaction 3 (plus topoisomerase) could be characterized. Illustrated here are samples of each class of molecule observed to constitute more than 10% of the molecules in at least one of the two reactions, with the percentages indicated for both the "plus-topo" and "minus-topo" conditions. (A) Unreplicated negatively supercoiled templates, showing the naturally occurring variation in the amount of supercoiling observed. (B) Rolling circle, conservative DNA synthesis from a small moving bubble. (C) Two supertwisted DNA molecules that contain a stalled replication bubble; the positive supertwisting of the nonreplicated part of the circular template produces a variety of plectonemic supercoils. (D) Nicked monomer circle (form II), the majority product in the presence of DNA topoisomerase. (E) Rolling circle, semiconservative DNA replication from a nicked, form II template. (F) DNA tangle. (G) Histogram comparing the percentages observed for each of the six classes of product, with (+) and without (–) topoisomerase present. The most abundant minor products not illustrated here were linear DNA molecules of roughly template length; these constituted ~10% of the total in both the plus-topo and minus-topo reactions and are thought to represent breakage products. Newly synapsed structures were detected in only minor amounts—as a circular double helix attached to a single-stranded, homologous primer that extends from a small D-loop (see Figure 8A). Scale bar indicates 100 nm.

As illustrated in the top pathway, this branch migration can displace Okazaki fragments formed inside the D-loop bubble, permitting a gradual elongation of the leading strand to continue. We believe that this process produces a small amount of conservative DNA synthesis in our in vitro system (molecule 2C in Figure 8). But unless specifically driven by a special DNA helicase appropriately positioned at the back of the D-loop bubble, this type of DNA synthesis would not be expected in cells, where DNA topoisomerase activity is always present.

In an attempt to better visualize the structure of the supertwisted DNA template molecules that contain stalled replication forks in Figure 7C, we examined the DNA products of the minus-topo reaction after treating them lightly with DNase to remove superhelical tension (see *Materials and Methods*). Here, we scored molecules with short tails whose topology was clear. The structures of three of these molecules are presented in Supplemental Figure S4, A–C. A total of 10 such molecules were analyzed to determine the size of the replication bubble in such molecules and the short lengths of DNA that extend from them. The schematic in Supplemental Figure S4D illustrates their general structure and defines lengths *W* and *X* for the DNA inside the replication bubble, plus lengths *Y* and *Y'* for the double-stranded DNA that is seen to extend from the opposite ends of this bubble. The measured lengths for *W*, *X*, *Y*, and *Y'* are presented for each of the 10 molecules in Supplemental Figure S4E. For this set of molecules, the mean value for $(W + X)/2$, the bubble size, is 1.36 ± 0.19 kb.

We attribute the large size of the replication bubbles in Supplemental Figure S4 (1.36 kb) to spontaneous DNA branch migration, a "random walk" process that would be expected after stopping our DNase treatment by Mg^{2+} chelation with EDTA (Panyutin and Hsieh, 1994). In a closed circular DNA molecule, the size of the replication bubble would only be about a fourth of this length (see, for example, Figure 7B). In fact, from Supplemental

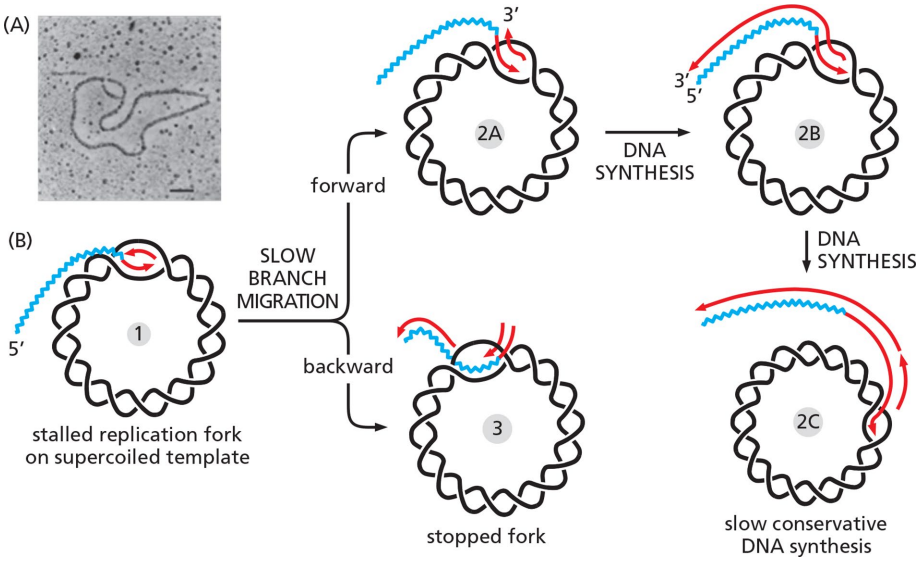

FIGURE 8: Some effects of branch migration on a covalently closed, circular DNA template molecule containing a replication bubble stalled by superhelical tension. In the absence of a DNA topoisomerase, the initial product of recombination-dependent DNA synthesis on a circular template is a supertwisted molecule with a stalled replication bubble. An electron micrograph of such a molecule with supertwists removed is presented in A. This is the same as Molecule 1 in B, where the 3″ end of a homologous single-stranded DNA primer (*blue*) has been extended a few hundred nucleotides by leading-strand DNA synthesis, and an Okazaki fragment has been synthesized on the other side of the D-loop. As indicated, this molecule can undergo branch migration. In the top pathway, a slow UvsX-catalyzed branch migration occurs behind the stalled replication bubble, displacing the 3′OH end of the Okazaki fragment that had been inside the replication bubble, while leaving the 3′ OH end of the extended primer paired with its template (Molecule 2A). The newly extruded end of the Okazaki fragment then primes DNA synthesis to make the homologous DNA primer double-stranded, creating molecule 2B. A slow process of rolling-circle replication from a small moving bubble may subsequently occur, creating molecule 2C, in which Okazaki fragments that were synthesized inside the replication bubble have been repeatedly displaced by UvsX-driven branch migration. The product is a double helix that has been synthesized conservatively. In the bottom pathway, branch migration occurs at both ends of the stalled replication bubble, causing the 3′ OH end of the extended primer to be displaced from its template, stopping DNA synthesis (molecule 3). In the absence of topoisomerase, electron microscopy reveals numerous products that resemble the molecules diagrammed here (e.g., see Figure 7C and Supplemental Figure S4).

Figure S4, the total length of the extended DNA primer chain can be estimated as 1.95 ± 0.24 kb. Because the initial primer length was 1.62 kb, DNA synthesis had been able to proceed for only 330 nucleotides on average in these 10 molecules, before the accumulation of superhelical tension stopped the recombination-dependent replication fork.

DISCUSSION

The prokaryotic protein complexes that function on DNA carry out processes that are very similar to those catalyzed by their relatives in eukaryotic cells, while being considerably less complex. In these "model systems," each task is generally performed by fewer protein subunits; in addition, one avoids the elaborate regulation of protein function that occurs in eukaryotes through protein phosphorylation and other types of covalent modification. And because bacteriophages in the wild have very short generation times and enormously competitive lifestyles, their sets of proteins central for viral success—such as those studied here—will have been finely tuned for optimal function through natural selection. For these reasons, mechanistic studies in prokaryotes will continue to provide information that is critical for our understanding of all other organisms.

To connect our findings to what has been discovered in other laboratories, we begin this discussion with a focus on the properties of the two T4 bacteriophage mediator proteins that function in the in vitro system used here, gp59 and UvsY, briefly relating them to analogous proteins in other DNA replication systems. Then we address the broader implications of this research, emphasizing the immense chemical sophistication that underlies the many protein–DNA interactions that are fundamental to life.

The gp59 and UvsY mediator proteins serve as both disassembly and assembly factors

The structures of both the gp59 and UvsY proteins have been determined by x-ray crystallography (Mueser *et al.*, 2000; Gajewski *et al.*, 2016), and their detailed modes of action have been analyzed by physicochemical techniques (Bleuit *et al.*, 2001; Zhang *et al.*, 2005; Liu *et al.*, 2006, 2013; Xu *et al.*, 2010; Branagan *et al.*, 2012, 2014; Benkovic and Spiering, 2017). These small proteins readily oligomerize: gp59 to form hexamers and UvsY to form heptamers. They bind both to single-stranded DNA and to gp32, and in their oligomerized forms they appear to use a "wrapping" process to remove a cooperatively-bound cluster of gp32 monomers from the DNA—simultaneously loading either a gp41 hexamer (in the case of gp59) or an assembly of UvsX monomers (in the case of UvsY) onto the freed-up stretch of nucleotides.

The gp59 is considerably larger than UvsY (26 vs. 15.8 kDa), and it contains binding sites that cause it to bind preferentially to forked DNA, positioning a bound gp32 molecule where it can nucleate the assembly of gp32 monomers on the displaced single strand of the D-loop (Hinerman *et al.*, 2012). In this position, the gp59 also "locks" any gp43 molecule bound to the invading 3′ end, thereby preventing this T4 DNA polymerase molecule from synthesizing DNA until the gp59 is repositioned by its loading of a gp41 hexamer as a ring around the DNA (Dudas and Kreuzer, 2005; Xi *et al.*, 2005; Benkovic and Spiering, 2017). Through this set of activities inside the D-loop, the gp59 mediator protein ensures that a semiconservative form of RDR produces the large amount of T4 DNA needed to fill T4 bacteriophage heads

One would assume that the UvsY mediator protein, like gp59, has the ability to load its partner UvsX at preferred sites on the DNA; however, this remains to be deciphered, and it would presumably require that UvsY bind additional proteins.

Mediator proteins with similar functions are found in many other organisms

As one would expect, proteins with functions analogous to those of gp59 and UvsY are required by many different types of cells. Although not a structural homologue, the best-studied gp59 analogue is priA, an *E. coli* protein that binds to the same type of fork

structure; unlike gp59, it contains a 3′ to 5′ helicase activity (Jones and Nakai, 2000). PriA functions as part of a larger protein complex that can load the *E. coli* hexameric replicative helicase, DNAB, onto DNA during replication restarts. Such restarts are needed during each bacterial cell cycle to overcome the unavoidable accidents that stall a replication fork (McGlynn and Lloyd, 2002; Mirkin and Mirkin, 2007), and they have been extensively studied in the *E. coli* in vitro system (Sandler and Marians, 2000; Xu and Marians, 2003; Gabbai and Marians, 2010; Liu *et al.*, 2011; Yeeles *et al.*, 2013).

Analogues to the UvsY recombination mediator protein in bacteria are the *E. coli* RecO, RecF, and RecR proteins, each of which can nucleate the cooperative assembly of RecA protein (the bacterial homologue to UvsX) on DNA single strands that are covered by *E. coli* SSB (the bacterial analogue to gp32). Not surprisingly, eukaryotic cells also contain mediator proteins with functions similar to those of gp59 and UvsY (reviewed in Yeeles *et al.*, 2013; Morrical, 2015; Korolov, 2017).

Large numbers of specific protein–protein interactions control how DNA functions in cells

We have thus far described only the specific protein–protein interactions in our in vitro system that involve mediator proteins. But it is clear that many other such specific interactions are also critical. As one example, the acidic C-terminal tail of gp32 interacts with gp59, gp43, UvsX, UvsY, dda, and gp61 in the set of proteins that we have employed (Morrical *et al.*, 1996). Because of such protein–protein interactions, three-dimensional folding is characteristic of DNA–protein assemblies (Echols, 1986), a fact omitted from standard cartoon drawings. Correspondingly, we know from previous work that the *E. coli* RecA protein cannot replace the UvsX protein, even though these homologues can catalyze essentially the same strand-exchange reactions (Formosa and Alberts, 1986).

Figure 9 illustrates how, in principle, recombination-dependent DNA synthesis can be directed to produce either a conservative or a semiconservative mode of DNA replication through a combination of specific inhibitory and specific stimulatory protein–protein interactions. In our case, the loading of the critical gp41 DNA helicase as a hexameric protein ring is specifically catalyzed at the front of the D-loop bubble by gp59, as previously explained, while being inhibited on the new single strand extruded from the D-loop by that strand's coating with cooperatively bound UvsX protein (see Figure 1). The resulting semiconservative type of RDR makes biological sense for T4 bacteriophage at late times of infection, since it efficiently generates the long concatemeric DNA structures on which empty T4 phage heads assemble to package a slightly more than unit-length final T4 chromosome (Mosig, 1983, 1987, 1998; Kreuzer, 2000).

In other cases, one might expect a different outcome, depending on the needs of the cell. In fact, DNA synthesis that resembles the conservative DNA synthesis illustrated in Figure 2 underlies the break-induced replication (BIR) that has thus far been observed in *Saccharomyces cerevisiae* (Saini *et al.*, 2013; Donnianni and Symington, 2013; Mayle *et al.*, 2015), as well as in mammalian cells—a process found to be abnormally enhanced in some cancers (Constantino *et al.*, 2014). This BIR process also differs from normal replication in requiring the Pol32/POLD3 subunit of eukaryotic DNA polymerase delta, as well as a special DNA helicase (Pif1 helicase, a T4 dda relative) that allows the D-loop bubble created by recombination-dependent DNA synthesis to continue to migrate for thousands of nucleotides. Clearly therefore, either outcome in Figure 2 is possible, evolution having presumably selected for the position and mechanism of helicase DNA loading that produces the best outcome for the cell.

Others have demonstrated that the ALT mechanism of telomere maintenance, which like BIR requires recombination-dependent DNA synthesis, occurs by a conservative mechanism (Roumelioti *et al.*, 2016). Any conservative form of DNA synthesis would seem to have the disadvantage of being inherently error-prone (Deem *et al.*, 2011), inasmuch as the mismatch repair system that removes most replication errors cannot function without a parental reference strand to guide it (Modrich, 2016). Perhaps for this reason, this type of replication normally appears to be limited to a few kilobases in S-phase, being terminated by mus81 nuclease cleavage (Mayle *et al.*, 2015).

The biochemical pathways used for DNA damage repair are known to be highly regulated (Murray and Carr, 2018). Because a study of BIR in the fission yeast *Schizosaccharomyces pombe* has revealed a form of RDR that proceeds semiconservatively during S-phase (Miyabe *et al.*, 2015), it may be that both conservative and semiconservative forms of RDR will occur in a eukaryote, depending on the precise circumstances.

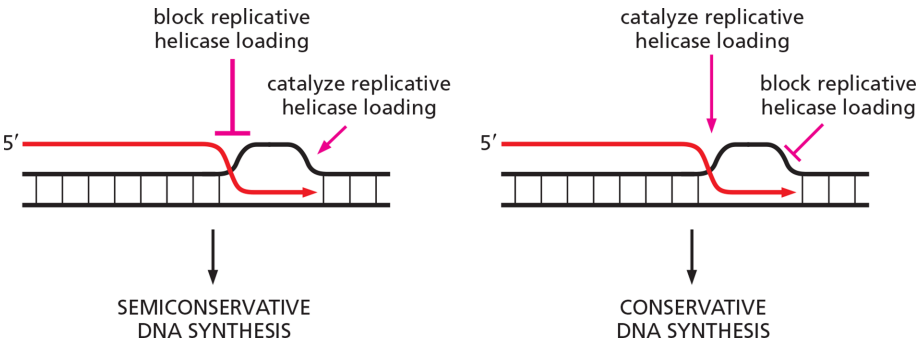

FIGURE 9: How cells use mediator proteins to control the outcome of recombination-dependent DNA replication (RDR). As described in the text, and observed in the experiments reported here, the loading of the gp41 DNA helicase on the displaced single strand is blocked by that strand's coating of UvsX protein, while being catalyzed at the front of the D-loop by the preferential binding of gp59 to the forked DNA and gp32 that is located there. As a result, the gp59 mediator protein loads gp41 only inside the D-loop. The gp41 then binds gp61 to produce semiconservative DNA replication. For the process of break-induced replication (BIR) thus far observed in *S. cerevisiae* and mammals, a different set of protein–protein interactions produces the opposite result, and DNA is replicated conservatively. Conservative DNA replication will be inherently error-prone, inasmuch as the mismatch repair systems that are essential for high replication fidelity cannot operate without the original parental strand to use as a reference.

Next steps

A controlled, site-specific assembly onto DNA of each of the many different protein complexes that function on DNA is central to biology. From genetics and pathway analyses, we know a large number of the essential components of these assemblies. But we will need much more in vitro biochemistry with purified proteins before scientists can claim to truly understand how DNA sequences are faithfully maintained by elaborate DNA repair processes, transmitted from one cell generation to the next by DNA replication and chromosome-sorting mechanisms, and used to express the

specific genetic information needed by a cell through highly selective DNA transcription events.

Much of cell chemistry is attributable to complexes of 10 or more proteins that may normally only interact weakly, being triggered to assemble into functional "protein machines" only when and where each machine is needed (Alberts, 1984, 1998). Understanding them requires reconstituting each process in a test tube with a mixture of highly purified proteins and nucleic acids, followed by the many biochemical manipulations and physical measurements required to uncover precise mechanisms. Even with respect to the specific small subset of reactions that we have studied here, much remains to be done. Thus, for example, inside the T4 bacteriophage-infected cell, in addition to dda and gp41, a third T4 DNA helicase, UvsW, is intimately involved in the reactions that enable replication forks to deal with lesions and replication accidents. UvsW is most notable for its ability to drive fork regression, as one elegant mode of DNA replication repair (Long and Kreuzer, 2008, 2009; Kreuzer and Brister, 2010; Kreuzer, 2013; Manosas *et al.*, 2012). But in some cases, UvsW functions with the same set of proteins that we have studied here. How might the addition of purified UvsW protein alter the reactions that we have reconstituted? When all three T4 DNA helicases are simultaneously present, where is each located and how does each affect the other? Because of extensive homologies with the helicases in other types of cells (Kerr *et al.*, 2007; He *et al.*, 2012; Mason *et al.*, 2014), the answers to such questions should contribute quite broadly to our understanding of cell biology.

MATERIALS AND METHODS

Assay for RNA-primed DNA synthesis on a circular, single-stranded DNA template

gp59 was examined for its ability to stimulate the de novo synthesis of DNA on a single-stranded, circular M13 DNA template in the presence of seven core T4 replication proteins and the T4 strand-exchange protein UvsX. In these assays the synthesis of RNA pentameric primers by the gp61 DNA primase (the 61-protein component of the primosome) is completely dependent on the presence of the gp41 DNA helicase (the 41-protein component of the primosome). All reaction mixtures were prepared on ice and contained assay buffer (66 mM potassium acetate, 33 mM Tris acetate, pH 7.8, 10 mM magnesium acetate, and 0.5 mM dithiothreitol), 100 μg/ml (or 50 μg/ml where indicated) HSA, ribo- and deoxyribonucleoside triphosphates (1 mM ATP, 1 mM GTP, and 0.2 mM each of CTP and UTP; 0.4 mM each of dATP and dGTP, 0.2 mM dCTP, and 0.2 mM [3H]dTTP at a specific activity of 1560 Ci/mol), M13 DNA template (3.3 μg/ml or 9.8 μM), an ATP regenerating system (10 mM creatine phosphate and 10 μg/ml creatine phosphate kinase, required to compensate for the high level of ATPase activity associated with UvsX protein), and T4 replication proteins (2.5 μg/ml gp43, 30 μg/ml gp44/gp62 protein complex, and 10 μg/ml gp45—constituting the DNA polymerase holoenzyme; 1 μg/ml gp61 and 21 μg/ml gp41—constituting the primosome). Present only when indicated were 62 μg/ml gp32, 100 μg/ml UvsX protein, and 0.6 μg/ml gp59. The assays were carried out at 37°C. Aliquots were taken at various times, synthesis was stopped by the addition of Na_3EDTA, pH 9.0, to a final concentration of 25 mM on ice, and the [3H]dTTP label incorporated into acid-insoluble DNA products was then determined (Formosa and Alberts, 1986). Results are expressed as nmol of total deoxyribonucleotide incorporated into DNA per ml of assay mixture.

Assay for recombination-dependent DNA synthesis

To examine the ability of gp59 to allow primosome function and Okazaki fragment synthesis (lagging strand synthesis) in a replication system initiated by genetic recombination, reaction mixtures were prepared on ice containing assay buffer (33 mM Tris acetate, pH 7.8, 66 mM potassium acetate, 10 mM magnesium acetate, and 0.5 mM dithiothreitol), 50 μg/ml HSA, ribo- and deoxyribonucleoside triphosphates (2 mM each of ATP and GTP, 0.2 mM each of CTP and UTP, 0.4 mM each of dGTP and dATP, 0.2 mM dCTP, and 0.15 mM [α-^{32}P]dTTP [at the specific activity given in the figure legends]), and the ATP regenerating system described previously. To reduce synthesis from nicks present in a minor fraction of template molecules, all reactions contained 2 units/ml T4 DNA ligase as well as 0.25 mM spermine and 0.15 mM spermidine. The following proteins were present in all reactions: 2.5 μg/ml gp43, 30 μg/ml gp44/gp62 protein complex, 10 μg/ml gp45, and 68 μg/ml gp32. The following proteins were present when indicated: 21 μg/ml gp41, 1 μg/ml gp61, 1 μg/ml gp59, 2 μg/ml dda protein, 21 μg/ml UvsX protein, 5 μg/ml UvsY protein, and 2 μg/ml of T4 type II DNA topoisomerase (gp39/gp52/gp60 complex; Liu *et al.*, 1979). The T4 UvsY protein nucleates UvsX protein assembly on single-stranded DNA, thus allowing a fivefold lower concentration of UvsX protein to be used (Morrical and Alberts, 1990).

When present, the double-stranded template was 20 μM (nucleotides) of the 7250 base pair M13MP19 DNA (1.38 nM as supercoiled circles or the *Bgl*II linearized form as indicated; see below). The single-stranded DNA primer was 2 μM (nucleotides) of the 1623 nucleotide, linear fragment (1.23 nM as fragments) cut from M13 single-stranded DNA circles with *Hae*III (see below). All components except for the DNA primer, the four deoxyribonucleoside triphosphates, the CTP and UTP, and 75% of the GTP and ATP were preincubated for 4 min at 37°C. Finally, the DNA primer and all of the missing nucleotides were added to start DNA synthesis. Portions of the reaction mixture were subsequently taken at various times and brought to 25 mM Na_3EDTA (using a pH 9.0 stock on ice) to stop DNA synthesis. The incorporation of the labeled dTTP into acid-insoluble DNA product is expressed as nmol (nucleotide)/ml reaction. DNA products were also analyzed for size and shape as described below.

DNA product analysis by agarose gel electrophoresis

In all cases, equal volumes of reaction mixture were compared on these gels. The analysis of DNA products by agarose gel electrophoresis under alkaline denaturing conditions (30 mM NaOH) is described in Barry and Alberts (1994). For the analysis of DNA products by neutral gel electrophoresis, samples were first made 0.4% in SDS and heated for 5 min at 65°C to denature DNA binding proteins. Samples were then adjusted to 10% sucrose, 0.03% bromophenol blue, and an additional 20 mM Na_3EDTA (pH 8) and loaded onto horizontal 0.8% agarose gels formed in neutral gel running buffer (50 mM Tris-Cl, pH 7.9, 40 mM sodium acetate, and 1 mM Na_3EDTA). The gels were run nonsubmerged at 20 V for 40 h, with the running buffer at both anode and cathode changed every 8–10 h. Upon completion, the gels were stained with ethidium bromide and the UV illuminated bands photographed to record the relative positions of standards—including forms I and II of plasmid M13MP19 DNA, the 40 kbp T7 DNA, and the linear double-stranded *Bst*EII and *Hin*dIII restriction fragments of bacteriophage lambda DNA. The gels are then acidified, dried, and autoradiographed as in Barry and Alberts (1994).

DNA product analysis by electron microscopy

Recombination-dependent DNA synthesis reactions were carried out as described above with HSA present at 50 μg/ml. Aliquots from reactions stopped with EDTA (see above) were diluted 20-fold to create a solution containing 0.5–1.0 μg/ml DNA, 40% formamide by

volume, and 0.1 mg/ml cytochrome *c* and were spread onto double-distilled water. The resulting cytochrome *c*–DNA-mixed film was picked up on grids covered with films prepared from 0.5% Formvar (Koller and Delius, 1984). The DNA-containing grids were stained by dipping them for 30 s in a 0.1 mg/ml uranyl acetate solution in 90% ethanol and, after drying, shadowed with platinum. DNA molecules were photographed with a Phillips EM 300 electron microscope using a 50-IA objective aperture and 60 kV accelerating voltage. A reasonably long stretch of a DNA molecule can usually be classified with confidence as either single- or double-stranded, inasmuch as the threadlike double-stranded DNA appears more rigid, smoother, and wider than the single-stranded DNA. However, due to this method's limited resolution, the position where the structure transitions from double- to single-stranded cannot be precisely determined.

DNase I nicking of the DNA products to remove superhelical tension

After 7 min of synthesis, the reaction was stopped with EDTA as described previously. The products of the minus-topoisomerase reaction (reaction 2, in Figure 6) were heated to 65°C for 10 min to denature the T4 replication and recombination proteins, and the DNA was separated from nucleotides and denatured protein on a BioSpin 30 column (BioRad), according to manufacturer's instructions. The DNA was recovered from this column in 40 mM Tris-Cl, pH 7.4, 10 mM $MgCl_2$, 20 µg/ml HSA. Bovine pancreatic DNase I (20 ng/ml) was added for a 5-min incubation at 37°C. The reaction was stopped with excess Na_3EDTA and the nicked DNA was prepared for electron microscopy as described above (see Supplemental Figure S4).

Reagents and enzymes

All restriction nucleases and most DNA-modifying enzymes (including T4 DNA ligase) were purchased from New England Biolabs in the early 1990s, when all of the reported experiments were performed. Nucleoside triphosphates were obtained from Pharmacia, creatine phosphate, creatine phosphate kinase, and DNase I were from Sigma, and human serum albumin (HSA) was from Worthington Biochemical Corporation. Radiolabeled compounds were obtained from Amersham. Other chemicals and biochemicals were obtained from Sigma unless specified otherwise. The T4 DNA topoisomerase was a generous gift from Ken Kreuzer (Duke University). The T4 bacteriophage UvsX and UvsY proteins were purified from overproducing strains as described in Morrical and Alberts (1990). The purified protein products of the cloned T4 genes 44/62 and 45 were prepared according to Morris *et al*. (1979) and the products of cloned T4 genes 32, 41, 43, 59 and 61 were purified as described in Barry and Alberts (1994).

All protein stocks used were free of contaminating nucleases, as judged by sensitive testing (Bittner *et al*., 1979). Nuclease testing of UvsX protein and gp32 was done at concentrations that left ~40% of the single-stranded DNA protein-free (see Figure 1 legend for stoichiometries). Protein concentrations were determined by Bradford assay, using bovine serum albumin (BSA) as the standard. The gp32 concentration was determined by absorption using A280 = 1.07/mg/ml. For the enzyme assays described below, small amounts of each protein were diluted using assay buffer (see below) supplemented with 100 µg/ml human serum albumin (HSA).

Nucleic acids

Circular single-stranded DNA from bacteriophage M13 was isolated as described for bacteriophage fd DNA in Burke *et al*. (1985). The 1623 nucleotide linear (*Hae*III) fragment of M13 single-stranded DNA was prepared and labeled with ^{32}P at the 5′-end using the alkaline phosphatase/T4 polynucleotide kinase method (Morrical and Alberts, 1990). Supercoiled (form I) DNA from bacteriophage M13MP19 was isolated as described in Morrical and Alberts (1990). M13MP19 DNA was linearized by restriction endonuclease cutting at the unique *Bgl*II site.

ACKNOWLEDGMENTS

We are indebted to Kenneth Kreuzer, Scott Morrical, and Jim Haber for their feedback and advice on earlier versions of this article, as well as to Nigel Orme for his skillful rendering of the figures. This work was supported by National Institutes of Health Grant GM24020.

REFERENCES

Alberts BM (1984). The DNA enzymology of protein machines. Cold Spring Harb Symp Quant Biol 49, 1–12.

Alberts BM (1998). The cell as a collection of protein machines: preparing the next generation of molecular biologists. Cell 92, 291–294.

Alberts BM, Barry J, Bedinger P, Formosa T, Jongeneel CV, Kreuzer KN (1983). Studies on DNA replication in the bacteriophage T4 in vitro system. Cold Spring Harb Symp Quant Biol 47, 655–668.

Alberts BM, Frey L (1970). T4 bacteriophage gene 32: a structural protein in the replication and recombination of DNA. Nature 227, 1313–1318.

Ando RA, Morrical SW (1998). Single-stranded DNA binding properties of the UvsX recombinase of bacteriophage T4: binding parameters and effects of nucleotides. J Mol Biol 283, 785–796.

Barry J, Alberts BM (1994). Purification and characterization of bacteriophage T4 gene 59 protein. A DNA helicase assembly protein involved in DNA replication. J Biol Chem 269, 33049–33062.

Benkovic SJ, Spiering MM (2017). Understanding DNA replication by the bacteriophage T4 replisome. J Biol Chem 292, 18434–18442.

Bittner M, Burke RL, Alberts BM (1979). Purification of the T4 gene 32 protein free from detectable deoxyribonuclease activities. J Biol Chem 254, 9565–9572.

Bleuit JS, Xu H, Ma Y, Wang T, Liu J, Morrical SW (2001). Mediator proteins orchestrate enzyme-ssDNA assembly during T4 recombination-dependent DNA replication and repair. J Biol Chem 279, 6077–6086.

Branagan AM, Klein JA, Jordan CS, Morrical SW (2014). Control of helicase loading in the coupled DNA replication and recombination systems of bacteriophage T4. J Biol Chem 289, 3040–3054.

Branagan AM, Maher RL, Morrical SW (2012) Assembly and dynamics of gp59-gp32-single-stranded DNA (ssDNA), a DNA helicase-loading complex required for recombination-dependent replication in bacteriophage T4. J Biol Chem 287,19070–19081.

Burke RL, Munn M, Barry J, Alberts BM (1985). Purification and properties of the bacteriophage T4 gene 61 RNA priming protein. J Biol Chem 260, 1711–1722.

Cha TA, Alberts BM (1986). Studies of the DNA helicase-RNA primase unit from bacteriophage T4. A trinucleotide sequence on the DNA template starts RNA primer synthesis. J Biol Chem 261, 7001–7010.

Clokie MR, Millard AD, Mann NH (2010). T4 genes in the marine ecosystem: studies of the T4-like cyanophages and their role in marine ecology. Virol J 7, 291.

Costantino L, Sotiriou SK, Rantala JK, Magin S, Mladenov E, Helleday T, Haber JE, Iliakis G, Kallioniemi OP, Halazonetis TD (2014). Break-induced replication repair of damaged forks induces genomic duplications in human cells. Science 343, 88–91.

Deem A, Keszthelyi A, Blackgrove T, Vayl A, Coffey B, Mathur R, Chabes A, Malkova A (2011). Break-induced replication is highly inaccurate. PLoS Biol 9, e1000594.

Delagoutte E, von Hippel PH (2005). Mechanistic studies of the T4 DNA (gp41) replication helicase: functional interactions of the C-terminal tails of the helicase subunits with the T4 (gp59) helicase loader protein. J Mol Biol 347, 257–275.

Donnianni RA, Symington LS (2013). Break-induced replication occurs by conservative DNA synthesis. Proc Natl Acad Sci USA 110, 13475–13480.

Dudas KC, Kreuzer KN (2005). Bacteriophage T4 helicase loader protein gp59 functions as gatekeeper in origin-dependent replication in vivo. J Biol Chem 280, 21561–21569.

Echols H (1986). Multiple DNA-protein interactions governing high-precision DNA transactions. Science 233, 1050–1056.

Englund PT (1971). The initial step of *in vitro* synthesis of deoxyribonucleic acid by the T4 deoxyribonucleic acid polymerase. J Biol Chem 246, 5684–5687.
Filée J, Tétart F, Suttle CA, Krisch HM (2005). Marine T4-type bacteriophages, a ubiquitous component of the dark matter of the biosphere. Proc Natl Acad Sci USA. 102, 12471–12476.
Formosa T, Alberts BM (1986). DNA synthesis dependent on genetic recombination: characterization of a reaction catalyzed by purified T4 proteins. Cell 47, 793–806.
Gabbai CB, Marians KJ (2010). Recruitment to stalled replication forks of the PriA DNA helicase and replisome-loading activities is essential for survival. DNA Repair (Amst) 9, 202–209.
Gajewski S, Webb MR, Galkin V, Egelman EH, Kreuzer KN, White SW (2011). Crystal structure of the phage T4 recombinase UvsX and its functional interaction with the T4 SF2 helicase UvsW. J Mol Biol 405, 65–76.
Gajewski S, Waddell MB, Vaithiyalingam S, Nourse A, Li Z, Woetzel N, Alexander N, Meiler J, White SW (2016). Structure and mechanism of the phage T4 recombination mediator protein UvsY. Proc Natl Acad Sci USA 113, 3275–3280.
Goulian M, Lucas ZJ, Kornberg A (1968). Enzymatic synthesis of deoxyribonucleic acid. XXV. Purification and properties of deoxyribonucleic acid polymerase induced by infection with phage T4. J Biol Chem 243, 627–638.
Griffith J, Formosa T (1985). The uvsX protein of bacteriophage T4 arranges single-stranded and double-stranded DNA into similar helical nucleoprotein filaments. J Biol Chem 260, 4484–4491.
Harris LD, Griffith J (1987). Visualization of the homologous pairing of DNA catalyzed by the bacteriophage T4 UvsX protein. J Biol Chem 262, 9285–9292.
He X, Byrd AK, Yun MK, Pemble CW4th, Harrison D, Yeruva L, Dahl C, Kreuzer KN, Raney KD, White SW (2012). The T4 phage SF1B helicase dda is structurally optimized to perform DNA strand separation. Structure 20, 1189–1200.
Hinerman JM, Dignam JD, Mueser TC (2012). Models for the binary complex of bacteriophage T4 gp59 helicase loading protein, gp32 single-stranded DNA-binding protein and ternary complex with pseudo-Y junction DNA. J Biol Chem 287, 18608–18617.
Hinton DM, Nossal NG (1987). Bacteriophage T4 DNA primase-helicase. Characterization of oligomer synthesis by T4 61 protein alone and in conjunction with T4 41 protein. J Biol Chem 262, 10873–10878.
Jensen DE, Kelly RC, von Hippel PH (1976). DNA "melting" proteins. II. Effects of bacteriophage T4 gene 32-protein binding on the conformation and stability of nucleic acid structures. J Biol Chem 251, 7215–7228.
Jing DH, Dong F, Latham GJ, von Hippel PH (1999). Interactions of bacteriophage T4-coded primase (gp61) with the T4 replication helicase (gp41) and DNA in primosome formation. J Biol Chem 274, 27287–27298.
Jones CE, Mueser TC, Dudas KC, Kreuzer KN, Nossal NG (2001). Bacteriophage T4 gene 41 helicase and gene 59 helicase-loading protein: a versatile couple with roles in replication and recombination. (2001). Proc Natl Acad Sci USA 98, 8312–8318.
Jones JM, Nakai H (2000). PriA and phage T4 gp59: factors that promote DNA replication on forked DNA substrates. Mol Microbiol 36, 519–527.
Kelch BA, Makino DL, O'Donnell M, Kuriyan J (2011). How a DNA polymerase clamp loader opens a sliding clamp. Science 334, 1675–1680.
Kerr ID, Sivakolundu S, Li Z, Buchsbaum JC, Knox LA, Kriwacki R, White SW (2007). Crystallographic and NMR analyses of UvsW and UvsW.1 from bacteriophage T4. J Biol Chem 282, 34392–34400.
Kodadek T (1990) The role of the bacteriophage gene 32 protein in homologous pairing. J Biol Chem 265, 20966–20969.
Kodadek T, Alberts BM (1987). Stimulation of protein-directed strand exchange by a DNA helicase. Nature 326, 312–314.
Kodadek T, Wong ML, Alberts BM (1988). The mechanism of homologous DNA strand exchange catalyzed by the bacteriophage T4 uvsX and gene 32 proteins. J Biol Chem 263, 9427–9436.
Koller B, Delius H (1984). Intervening sequences in chloroplast genomes. Cell 36, 613–622.
Korolov S (2017). Advances in structural studies of recombination mediator proteins. Biophys Chem 225, 27–37.
Kreuzer KN (2000). Recombination-dependent DNA replication in phage T4. Trends Biochem Sci 25, 165–173.
Kreuzer KN (2013). DNA damage responses in prokaryotes: regulating gene expression, modulating growth patterns, and manipulating replication forks. Cold Spring Harb Perspect Biol 5, a012674.
Kreuzer KN, Brister JR (2010). Initiation of bacteriophage T4 DNA replication and replication fork dynamics: a review in the Virology Journal series on bacteriophage T4 and its relatives. Virol J 7, 358.
Lee W, Jose D, Phelps C, Marcus AH, von Hippel PH (2013). A single-molecule view of the assembly pathway, subunit stoichiometry, and unwinding activity of the bacteriophage T4 primosome (helicase-primase) complex. Biochemistry 52, 3157–3170.
Liu CC, Alberts BM (1980). Pentaribonucleotides of mixed sequence are synthesized and efficiently prime de novo DNA chain starts in the T4-bacteriophage DNA-replication system. Proc Natl Acad Sci USA 77, 5698–5702.
Liu CC, Alberts BM (1981). Characterization of RNA primer synthesis in the T4 bacteriophage in vitro DNA replication system. J Biol Chem 256, 2821–2829.
Liu CC, Burke RL, Hibner U, Barry J, Alberts BM (1979). Probing DNA replication mechanisms with the T4 bacteriophage in vitro system. Cold Spring Harb Symp Quant Biol 43, 469–487.
Liu J, Berger CL, Morrical SW (2013). Kinetics of presynaptic filament assembly in the presence of single-stranded DNA binding protein and recombination mediator protein. Biochemistry 52, 7878–7889.
Liu J, Bond JP, Morrical SW (2006). Mechanism of presynaptic filament stabilization by the bacteriophage T4 UvsY recombination mediator protein. Biochemistry 45, 5493–5502.
Liu J, Ehmsen KT, Heyer WD, Morrical SW (2011). Presynaptic filament dynamics in homologous recombination and DNA repair. Crit Rev Biochem Mol Biol 46, 240–270.
Liu J, Morrical SW (2010). Assembly and dynamics of the bacteriophage T4 homologous recombination machinery. Virol J 7, 357.
Liu LF, Liu CC, Alberts BM (1979). T4 DNA topoisomerase: a new ATP-dependent enzyme essential for the initiation of T4 bacteriophage DNA replication. Nature 281, 456–461.
Long DT, Kreuzer KN (2008). Regression supports two mechanisms of fork processing in phage T4. Proc Natl Acad Sci USA 13, 6852–6857.
Long DT, Kreuzer KN (2009). Fork regression is an active helicase-driven pathway in bacteriophage T4. EMBO Rep 10, 394–399.
Luder A, Mosig G (1982). Two alternative mechanisms for initiation of DNA replication forks in bacteriophage T4: priming by RNA polymerase and by recombination. Proc Natl Acad Sci USA 79, 1101–1105.
Ma Y, Wang T, Villemain JL, Giedroc DP, Morrical SW (2004). Dual functions of single-stranded DNA-binding protein in helicase loading at the bacteriophage T4 DNA replication fork. J Biol Chem 279, 19035–19045.
Manosas M, Perumal SK, Croquette V, Benkovic SJ (2012). Direct observation of stalled fork restart via fork regression in the T4 replication system. Science 338, 1217–1220.
Mason AC, Rambo RP, Greer B, Pritchett M, Tainer JA, Cortez D, Eichman BF (2014). A structure-specific nucleic acid-binding domain conserved among DNA repair proteins. Proc Natl Acad Sci USA 111, 7618–7623.
Mayle R, Campbell IM, Beck CR, Yu Y, Wilson M, Shaw CA, Bjergbaek L, Lupski JR, Ira G (2015). Mus81 and converging forks limit the mutagenicity of replication fork breakage. Science 349, 742–747.
McGlynn P, Lloyd RG (2002). Recombinational repair and restart of damaged replication forks. Nat Rev Mol Cell Biol 3, 859–870.
Mirkin EV, Mirkin SM (2007). Replication fork stalling at natural impediments. Microbiol Mol Biol Rev 71, 13–35.
Miyabe I, Mizuno K, Keszthelyi A, Daigaku Y, Skouteri M, Mohebi S, Kunkel TA, Murray JM, Carr AM (2015). Polymerase δ replicates both strands after homologous recombination-dependent fork restart. Nat Struct Mol Biol 22, 932–938.
Modrich P (2016). Mechanisms in *E. coli* and human mismatch repair (Nobel Lecture). Angew Chem Int Ed Engl 55, 8490–8501.
Morrical SW (2015). DNA-pairing and annealing processes in homologous recombination and homology-directed repair. Cold Spring Harb Perspect Biol 7, a016444.
Morrical SW, Alberts BM (1990). The UvsY protein of T4 modulates recombination-dependent DNA synthesis in vitro. J Biol Chem 265, 15096–15103.
Morrical SW, Beernink HT, Dash A, Hempstead K (1996). The gene 59 protein of bacteriophage T4. Characterization of protein-protein interactions with gene 32 protein, the T4 single-stranded DNA binding protein. J Biol Chem 271, 20198–20207.
Morrical SW, Hempstead K, Morrical MD (1994). The gene 59 protein of bacteriophage T4 modulates the intrinsic and single-stranded DNA-stimulated ATPase activities of gene 41 protein, the T4 replicative DNA helicase. J Biol Chem 269, 33069–33081.
Morrical SW, Wong ML, Alberts BM (1991). Amplification of snap-back DNA synthesis reactions by the UvsX recombinase of bacteriophage T4. J Biol Chem 266, 14031–1403.

Morris CF, Hama-Inaba H, Mace D, Sinha NK, Alberts BM (1979). Purification of the gene 43, 44, 45, and 62 proteins of the bacteriophage T4 DNA replication apparatus. J Biol Chem 254, 6787–6796.
Morris CF, Sinha NK, Alberts BM (1975). Reconstruction of bacteriophage T4 DNA replication apparatus from purified components: rolling circle replication following de novo chain initiation on a single-stranded circular DNA template. Proc Natl Acad Sci USA 72, 4800–4804.
Mosig G (1983). Relationship of T4 DNA replication and recombination. In: Bacteriophage T4, Vol. 1, ed. CK Mathews, EM Kutter, G Mosig, and PB Berget, Washington, DC: American Society for Microbiology, 120–130.
Mosig G (1987). The essential role of recombination in phage T4 growth. Annu Rev Genet 21, 347–371.
Mosig G (1998). Recombination and recombination-dependent DNA replication in bacteriophage T4. Annu Rev Genet 32, 379–413.
Mueser TC, Jones CE, Nossal NG, Hyde CC (2000). Bacteriophage T4 gene 59 helicase assembly protein binds replication fork DNA. The 1.45-Å resolution crystal structure reveals a novel helical two-domain fold. J Mol Biol 296, 597–612.
Murray JM, Carr AM (2018). Integrating DNA damage repair with the cell cycle. Curr Opin Cell Biol, 52 120–125.
Nossal NG (1994). The bacteriophage T4 DNA replication fork. In: Bacteriophage T4, Vol. 1, ed. CK Mathews, EM Kutter, G Mosig, and PB Berget, Washington, DC: American Society for Microbiology, 43–53.
Nossal NG, Alberts BM (1983). The mechanism of DNA replication catalyzed by purified bacteriophage T4 DNA replication proteins. In: Bacteriophage T4, Vol. 1, ed. CK Mathews, EM Kutter, G Mosig, and PB Berget, Washington, DC: American Society for Microbiology, 71–81.
Nossal NG, Peterlin BM (1979). DNA replication by bacteriophage T4 proteins. The T4 43, 32, 44–62, and 45 proteins are required for strand displacement synthesis at nicks in duplex DNA. J Biol Chem 254, 6032–6037.
Panyutin IG, Hsieh P (1994). The kinetics of spontaneous DNA branch migration. Proc Natl Acad Sci USA 91, 2021–2025.
Roumelioti FM, Sotiriou SK, Katsini V, Chiourea M, Halazonetis TD, Gagos S (2016). Alternative lengthening of human telomeres is a conservative DNA replication process with features of break-induced replication. EMBO Rep 17, 1731–1737.
Saini N, Ramakrishnan S, Elango R, Ayyar S, Zhang Y, Deem A, Ira G, Haber JE, Lobachev KS, Malkova A (2013). Migrating bubble during break-induced replication drives conservative DNA synthesis. Nature 502, 389–392.
Sandler SJ, Marians KJ (2000). Role of PriA in replication fork reactivation in *Escherichia coli*. J Bacteriol 182, 9–13.
Shah DB (1976). Replication and recombination of gene 59 mutant of bacteriophage T4D. J Virol 17, 175–182.
Sinha NK, Morris CF, Alberts BM (1980). Efficient in vitro replication of double-stranded DNA templates by a purified T4 bacteriophage replication system. J Biol Chem 255, 4290–4303.
Strauss BS (2017). A physicist's quest in biology: Max Delbrück and "complementarity." Genetics 206, 641–650.
Suttle CA (2007). Marine viruses—major players in the global ecosystem. Nat Rev Microbiol 5, 801–812.
Wang JC (1969). Degree of superhelicity of covalently closed cyclic DNA's from *Escherichia coli*. J Mol Biol 43, 263–272.
Xi J, Zhang Z, Zhuang Z, Yang J, Spiering MM, Hammes GG, Benkovic SJ (2005). Interaction between the T4 helicase loading protein (gp59) and the DNA polymerase (gp43): unlocking of the gp59-gp43-DNA complex to initiate assembly of a fully functional replisome. Biochemistry 44, 7747–7756.
Xu H, Beernink HT, Morrical SW (2010). DNA-binding properties of T4 UvsY recombination mediator protein: polynucleotide wrapping promotes high-affinity binding to single-stranded DNA. Nucleic Acids Res 38, 4821–4833.
Xu L, Marians KJ. (2003). PriA mediates DNA replication pathway choice at recombination intermediates. Mol Cell 1, 817–826.
Yeeles JT, Poli J, Marians KJ, Pasero P (2013). Rescuing stalled or damaged replication forks. Cold Spring Harb Perspect Biol 5, a012815.
Yonesaki T (1984). The purification and characterization of gene 59 protein from bacteriophage T4. J Biol Chem 269, 1284–1289.
Yonesaki T, Minagawa T (1985). T4 phage gene uvsX product catalyses homologous DNA pairing. EMBO J 4, 3321–3327.
Zhang Z, Spiering MM, Trakselis MA, Ishmael FT, Xi J, Benkovic SJ, Hammes GG (2005). Assembly of the bacteriophage T4 primosome: single-molecule and ensemble studies. Proc Natl Acad Sci USA 102, 3254–3259.